sustainability

MDPI

Article

Sorption of Cd^{2+} and Pb^{2+} on Aragonite Synthesized from Eggshell

Lulit Habte [1,2], Natnael Shiferaw [3], Mohd Danish Khan [1,2], Thenepalli Thriveni [2] and Ji Whan Ahn [2,*]

1 Resources Recycling Department, University of Science and Technology (UST), 217, Gajeong-ro, Yuseong-gu, Daejeon-34113, Korea; luna1991@ust.ac.kr (L.H.); danish0417@ust.ac.kr (M.D.K.)
2 Center for Carbon Mineralization, Mineral Resources Research Division, Korea Institute of Geosciences and Mineral Resources (KIGAM), 124 Gwahak-ro, Yuseong-gu, Daejeon-34132, Korea; thenepallit@rediffmail.com
3 International Center for Urban Water Hydroinformatics Research & Innovation, 169 Gaetbeol, yeonsu-gu, Incheon, Korea; natlulit@gmail.com
* Correspondence: ahnjw@kigam.re.kr; Tel.: +8-868-3578

Received: 31 December 2019; Accepted: 4 February 2020; Published: 6 February 2020

Abstract: In the present work, waste eggshells were used as a precursor for the synthesis of aragonite crystals through the wet carbonation method. Cadmium (Cd^{2+}) and lead (Pb^{2+}) were removed by the synthesized aragonite from synthetic wastewater. The influence of initial solution pH, contact time, Cd^{2+} and Pb^{2+} concentration, and sorbent dosage were evaluated. The major sorption was observed in the first 100 mins and 360 mins for $Pb^{2+}$and Cd^{2+} respectively reaching sorption equilibrium at 720 mins (12 hr). The sorption capacity toward Pb^{2+} was much higher than toward Cd^{2+}. Both heavy metals displayed high sorption capacities at initial pH 6. The pseudo-second-order kinetic model fits well with the experimental data with a higher correlation coefficient R^2. Two isotherm models were also evaluated for the best fit with the experimental data obtained. Langmuir isotherm best fits the sorption of the metals on aragonite synthesized from eggshells. X-ray diffraction (XRD) and Scanning electron microscopy (SEM) results of sorbent after sorption showed that the mechanism of sorption was dominated by surface precipitation. Therefore, aragonite crystals synthesized from waste eggshells can be a potential substitute source for the removal of Cd^{2+} and Pb^{2+} from contaminated water.

Keywords: Aragonite; eggshells; lead; cadmium; sorption

1. Introduction

Solid waste management, being a current vital issue, is a huge burden regarding sustainability. Indecorous management of solid wastes such as municipal, industrial, and hazardous waste are emerging threats to the environment. The rapid rise in population resulted in an increase in food waste such as eggshell, which is one of the solid wastes available in abundance with serious environmental problems. Globally, approximately 5.92 million tonnes of waste eggshell are generated per year [1]. These waste eggshells have been dumped into landfills without further treatment, causing several environmental consequences [2]. The waste is mainly made up of calcium carbonate ($CaCO_3$) with minor impurities, which has been used in further applications as a source of calcium supplements [3–5]. However, the effect of impurities has been minimized with further treatments such as chemical treatment and physical treatment [6,7].

Cadmium (Cd^{2+}) and lead (Pb^{2+}) are prevalent heavy metals used in industries such as the electroplating industry, metal refining industry, and battery industry [8]. Waterbodies are contaminated by heavy metals through industrial wastewater. Cd^{2+} and Pb^{2+} are considered threats to the environment

due to their cause of acute and chronic damage to human and aquatic life [9]. Lead causes disorder of the brain, anemia, kidney disease, and palsy [9]. Cadmium causes kidney damage, proteinuria, and lung cancer [10]. Therefore, the release of these toxic heavy metals to water bodies should be controlled.

Numerous methods have emerged for removing dissolved heavy metals from contaminated water bodies. Adsorption [6,11–18], chemical precipitation [19], advanced Fenton-chemical precipitation [20], layered double hydroxide precipitation [21], physico-chemical treatment [22], electrocoagulation [23], flotation [24], ion exchange [25], and reverse osmosis [26] are some of these methods. Adsorption is a common method due to better performance, ease of operation, and low cost. Different adsorbents such as waste adsorbents are becoming popular for waste management and creating a sustainable world. The most commonly used waste adsorbents are waste bivalve shells [27,28]. Currently, waste eggshell is also well used for the treatment of wastewater [6,17,29,30].

Calcium carbonate is one of the abundant natural materials that exist in three main polymorphs: calcite, aragonite, and vaterite [31]. Aragonite is one form of the three polymorphics of $CaCO_3$. It has a needle shape morphology with more compact and denser properties [32]. Several studies reported that aragonite is an effective adsorbent with high adsorption capacity toward heavy metals [27,33,34]. Moreover, other studies have found that aragonite exhibited higher adsorption capacity toward Cd^{2+}, whereas calcite had higher absorption capacity toward Pb^{2+} [27,35,36]. However, the adsorption capacity of aragonite toward Pb^{2+} was also comparable to that of calcite [27]. The performance of the synthesized aragonite toward both metals was investigated in this study.

The objective of the present work is to study the potential use of synthesized aragonite crystals from eggshells in the sorption of Cd^{2+} and Pb^{2+} from synthetic wastewater. The study targeted these two metals due to their large-scale presence in industrial wastewater. The influence of various factors on the sorption capacity of synthesized aragonite was explored. The sorption kinetics and isotherm were also systematically studied.

2. Experimental

2.1. Materials

Waste eggshell was obtained from the Korean Institute of Geoscience and Minerals (KIGAM) campus restaurant in Daejeon, South Korea. Sodium hydroxide with 97% purity, hydrochloric acid with 35–37% concentration, nitric acid with 69–70% purity, $Pb(NO_3)_2$ with 99.95% purity, $Cd(NO_3)_2{\cdot}4\ H_2O$ with 98% purity, and magnesium chloride hexahydrate with 98% purity were all purchased from Junsei Chemicals Ltd., Seoul, Korea, while carbon dioxide with 99.9% purity was provided by Jeil Trading CO., Ltd Company, Seoul, Republic of Korea.

2.2. Synthesis of Sorbent (Aragonite)

Calcium hydroxide ($Ca(OH)_2$) synthesized from waste eggshell was used as a precursor. The synthesis of $Ca(OH)_2$ was described in detail in previous work [37]. The wet carbonation method was used for the synthesis of aragonite. One liter aqueous solution of calcium hydroxide and magnesium chloride hexahydrate was prepared with a molar ratio of 1:8 (Mg: Ca). The suspension was stirred continuously at 400 rpm at 80 °C, and pH was monitored continuously. After the stabilization of pH, CO_2 gas was introduced to the suspension at 50 mL/min flow rate. The solution pH gradually decreases with the injection of carbon dioxide. The reaction process comes to an end when the pH consistency of the suspension was observed. The synthesized aragonite was then washed, filtered and dried.

2.3. Sorption Experiments

$Pb(NO_3)_2$ and $Cd(NO_3)_2\ {\cdot}4\ H_2O$ were dissolved in de-ionized water at specified concentrations to prepare synthetic solutions in a sealed 1000 mL glass vessel. Then, 200 mL of the stock solutions were pre-equilibrated for 24 h prior to the addition of the adsorbent at room temperature. A specified amount

of aragonite was added to the flasks. Then, samples were analyzed for remaining metal concentrations by ICP-OES which were collected at designated time intervals. The initial pH adjustments were made by HNO_3 (0.1 M) or NaOH (0.1 M) solutions. The influence of three parameters on the adsorption capacity have been studied—adsorbent dosage (0.1 g/L–0.5 g/L), initial pH (2–6), and initial metal concentration (10 mg/L–100 mg/L). First, the dosage effect was investigated with Cd^{2+} and Pb^{2+} concentration of 100 mg/L and solution pH (~5.8). A dosage with optimum removal efficiency was selected to study the influence of the other parameters. The influence of initial pH was then studied with Cd^{2+} and Pb^{2+} concentration of 100 mg/L and the previously selected dosage of aragonite. Finally, the influence of Cd^{2+} and Pb^{2+} concentration was investigated with the previously selected pH and dosage. The selected optimum conditions were used for the sorption kinetics and isotherm studies. Table 1 presents detailed experimental conditions.

Table 1. The influence of sorbent dosage, initial pH, and Cd^{2+} and Pb^{2+} concentration on the sorption of metals on aragonite synthesized from eggshell at different experimental conditions.

Parameters	Values	Adsorption Capacity (mg/g)		Removal Efficiency (%)		Experimental Condition
		Cd^{2+}	Pb^{2+}	Cd^{2+}	Pb^{2+}	
Sorbent dosage (g/L)	**0.1**	500	987.5	41.7	97.5	Initial pH = 5.8 and Cd^{2+} and Pb^{2+} concentration = 100 mg/L
	0.2	400	501	66.7	99	
	0.3	333.3	335.8	83.3	99.5	
	0.4	256.3	251.9	85.4	99.5	
	0.5	185	202	86	99.8	
Initial pH	2	0	0	0	0	Sorbent dosage = 0.3 g/L and Cd^{2+} and Pb^{2+} = 100 mg/L
	3	175	276.7	43.8	82	
	4	316.7	334.2	79.2	99	
	5	325	335	81.3	99.3	
	6	333.3	335.8	83.3	99.5	
Cd^{2+} and Pb^{2+} concentration (mg/L)	10	34.2	35.8	80.4	99.1	Sorbent dosage = 0.3 g/L and Initial pH = 6
	50	179.2	185.8	81.1	99.3	
	100	333.3	335.8	83.3	99.5	

The percentage of ion (%) removal was determined at various experimental conditions by Equation (1).

$$\text{Removal } (\%) = \frac{\text{Co} - \text{Ct}}{\text{Co}} * 100 \quad (1)$$

where C_o and C_t are initial and final concentration in mg/L, respectively.

The adsorption capacities were also calculated using Equation (2).

$$\text{Adsorption capacity, } qe\ (\text{mg/g}) = \frac{(\text{Co} - \text{Ce})\text{V}}{\text{S}} \quad (2)$$

where C_o is the initial and C_e is the equilibrium metal concentration in mg/L, V is solution volume in liters, and S is the amount of adsorbent used in grams.

2.4. Characterization

Mineralogical and crystallographic phases of synthesized aragonite were investigated by powder X-ray diffraction (XRD) with 2θ ranging from 10° to 90° (BD2745N, Rigaku, Tokyo, Japan). Scanning electron microscopy (SEM), (JSM-6330F, JEOL. Co. Ltd., Tokyo, Japan) was used for crystal structure, shape, and morphological analysis of the synthesized aragonite. The specific surface area of the sorbent was conducted by Brunauer–Emmett–Teller (BET) (Quadrasorb SI, Quantachrome Instruments, Florida, USA). A Particle size analyzer (Malvern Zetasizer Nano ZS90, Cambridge, United

Kingdom) was used for particle size distribution analysis. A surface charge study was conducted through zeta potential analysis (Otsuka ELS-Z, Osaka, Japan). The pH of the solution was measured by Orion Versa Star Pro (ThermoFisher Scientific, Waltham, MA, USA) pH meter with a glass electrode. Inductive coupled plasma-optical emission spectroscopy (ICP-OES) (PerkinElmer, Inc. Waltham, MA, USA) was used for the measurement of metal concentrations.

3. Result and Discussion

3.1. Characterizations of Sorbent

Crystal structures and mineralogical phases of waste eggshell and synthesized aragonite were determined by powder XRD. As illustrated in Figure 1a, the raw eggshell has a major phase of rhombohedral calcite with a space group *R-3c* (Space Group No. 167; JCPDS PDF Card No.86-0174) appeared at 2θ= 29.48. Figure 1b represents the XRD patterns of aragonite synthesized from eggshells. All the peaks of synthesized sorbent resembled aragonite phase, which implies that the transformation of calcite to a high grade (with minor calcite) aragonite crystals can be obtained from waste eggshell through wet carbonation.

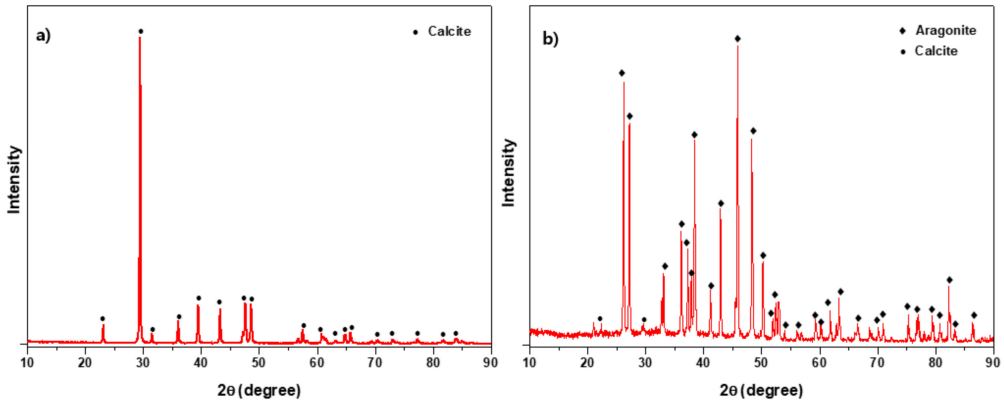

Figure 1. X-ray diffraction patterns of (**a**) raw eggshell and (**b**) aragonite synthesized from eggshell.

Figure 2 represents the surface morphology of the synthesized aragonite. Needle-shaped aragonite particles with an average aspect ratio of 21 were successfully synthesized.

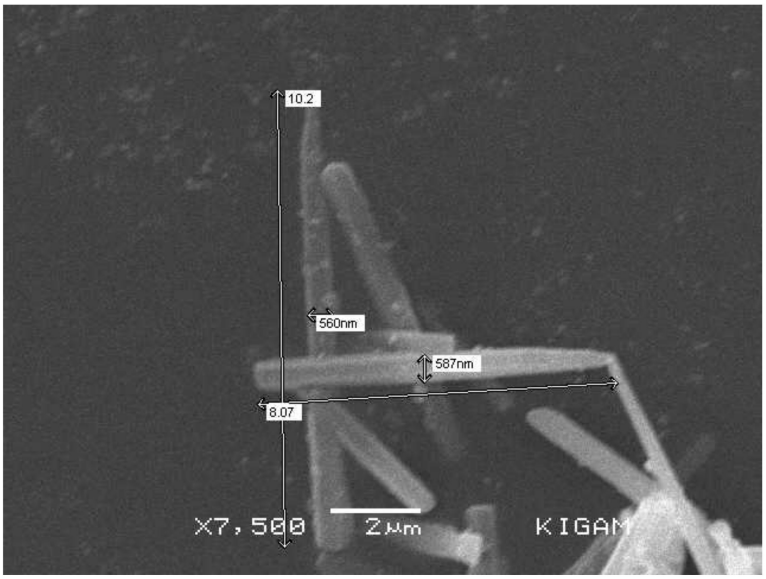

Figure 2. Scanning electron microscopy images of synthesized aragonite from eggshell.

The particle size distribution of aragonite synthesized from eggshell was found in the range of 10–45 μm, with the highest peak at ~ 20 μm, as can be seen in Figure 3. The presence of nitrogen compounds from amino acids/proteins aid the synthesis of smaller particle size distribution [38,39]. The specific surface area of aragonite synthesized from eggshell was determined as high as ~ 18.7 m^2g^{-1} due to the smaller particle size obtained. Specific surface area increases as particle size decreases, resulting in higher adsorption capacity. Therefore, the higher surface area of the synthesized aragonite aids the performance of the sorbent.

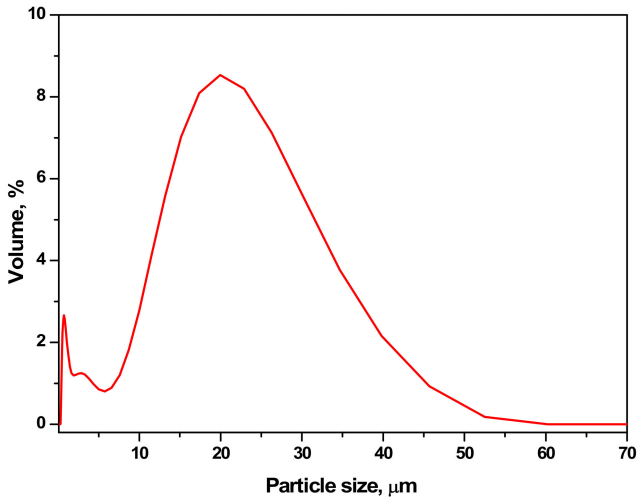

Figure 3. The particle size distribution of aragonite synthesized from eggshell.

Zeta potential is the key parameter of a sorbent in the adsorption process. It informs the characteristics of the surface charge of particles suspended in an aqueous medium. Figure 4 illustrates the zeta potential values of synthesized aragonite with varied pH. The particles started to dissolve as pH < 6. Furthermore, no positive charge was found on the surface of the synthesized aragonite. The negative zeta potential values of the adsorbent show the suitability of adsorption of positively charged metals.

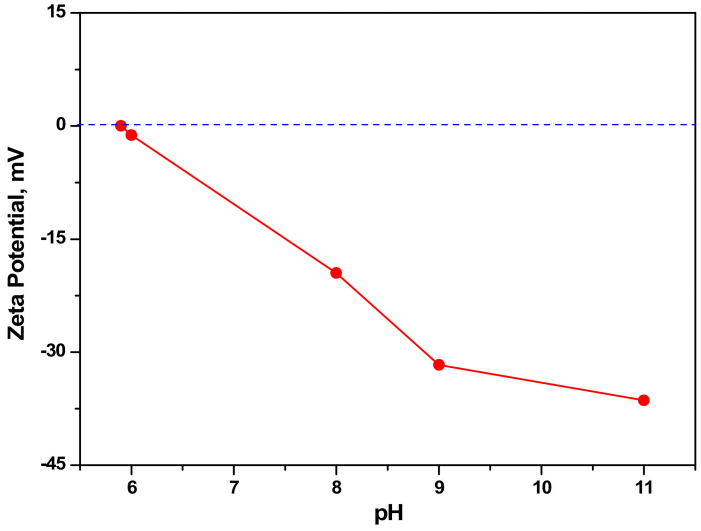

Figure 4. Zeta potential values of synthesized aragonite from eggshell.

3.2. Influence of Contact Time and Sorption Kinetics

As presented in Figure 5, the sorption phase was very fast initially due to the available active sorption sites on the sorbent followed by a slow sorption phase, indicating the active sites being occupied by the sorbed metals [27]. The major sorption took place in the first 100 mins for Pb^{2+} and 360 mins for Cd^{2+}, and both metals reached sorption equilibrium at 12 h. This can be explained by the hydration energies of the two metals. The hydration energy of Cd^{2+} and Pb^{2+} are −1807 KJ/mol and −1481 KJ/mol respectively as given later in Table 4. The slow sorption process of Cd^{2+} is due to the higher hydration energy than Pb^{2+}, which tends to stay in the solution.

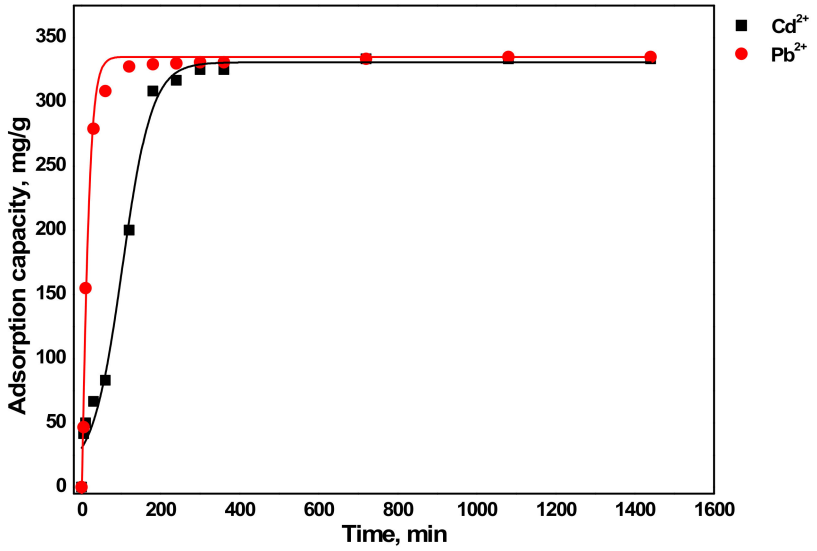

Figure 5. Influence of contact time on sorption of metals by aragonite.

The sorption mechanism was investigated through modelling the kinetics of metals sorption on synthesized aragonite with the first and pseudo-second-order kinetic models as given in Equations (3) and (4), respectively.

$$\log(qe - qt) = \log(qe) - \frac{K1}{2.303}t \quad (3)$$

$$\frac{t}{qe} = \frac{1}{K2 * qe^2} + \frac{1}{qe}t \quad (4)$$

where k_1 (min^{-1}) and k_2 (g mg^{-1} min^{-1}) are first and second-order rate constants respectively, t (min) is the time duration of sorption, and qe (mg/g) and qt (mg/g) are adsorption capacity at equilibrium and time t, respectively.

Figure 6 presents the first order and pseudo-second-order kinetic model fitted to the experimental data. The goodness of fit reports whether a model matches well with the experimental data or not. The correlation coefficient R^2 value, which is considered as a criterion for determination of good fit and other parameters, is given in Table 2. The R^2 values of the first-order kinetic model were observed lower. Moreover, the adsorption capacity of metals (especially Pb^{2+}) calculated from the model was much lower than those determined from the experiment. On the contrary, the R^2 values with the pseudo-second-order kinetic model were estimated as 0.986 for Cd^{2+} and 0.999 for Pb^{2+} which were much higher than the R^2 values with the first-order kinetic model. Besides, the estimated adsorption capacities (q_e) of the model were very close to those obtained from experiments. Therefore, the pseudo-second kinetic model is a good match for the sorption process, indicating that the sorption mechanism is mainly dominated by chemisorption.

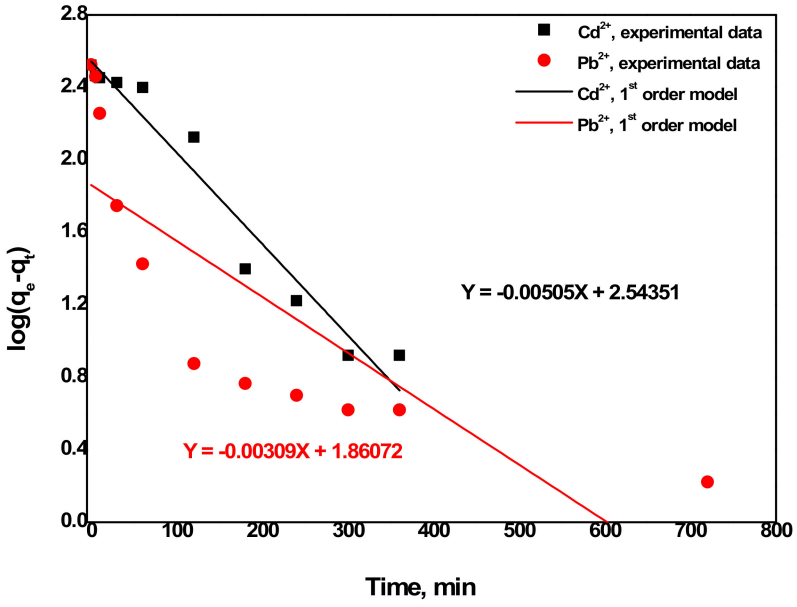

a)

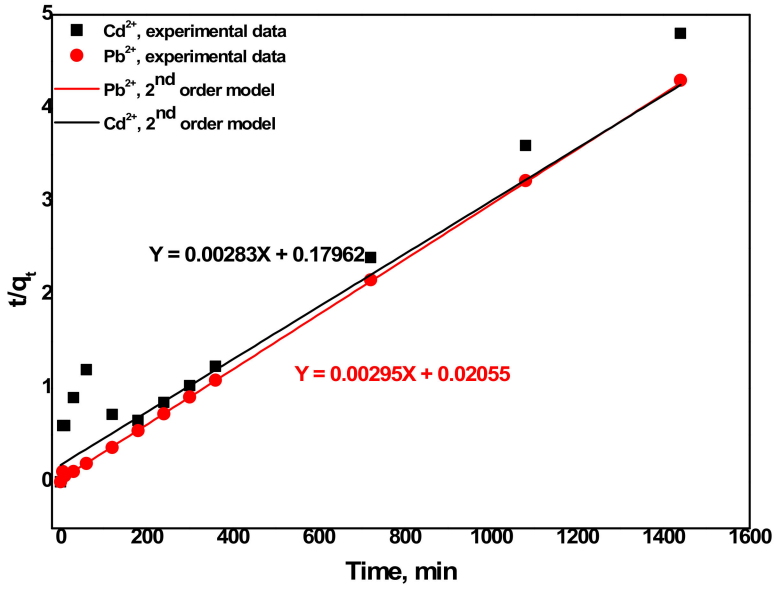

b)

Figure 6. (**a**) First-order and (**b**) pseudo-second-order kinetic models of metals sorption on aragonite.

Table 2. Kinetic model parameters of metals sorption on aragonite.

Metal	First-Order Parameters			Pseudo Second-Order Parameterser Parameters		
	q_e (mg g^{-1})	K_1 (min^{-1})	R^2	q_e (mg g^{-1})	K_2 (g mg^{-1} min^{-1})	R^2
Cd^{2+}	349.55	0.01163	0.951	353.36	4.46*10^−5	0.986
Pb^{2+}	72.56	7.11*10^−3	0.617	338.98	4.23*10^−4	0.999

3.3. Influence of Sorbent Dosage

The adsorption capacity of a sorbent toward the sorbate is directly affected by an indispensable parameter, sorbent dosage. It determines the amount of sorbent needed for the removal of a certain amount of contaminants. The effect was investigated by varying the amount of synthesized aragonite from 20 to 100 mg in 200 mL heavy metal-containing solution with Cd^{2+} and Pb^{2+} concentration of 100 mg/L at solution pH 5.8. As outlined in Figure 7, both the removal efficiency and sorption capacity of Cd^{2+} was much lower than that of Pb^{2+}. This result was also obtained from the previous study on biosorption of Pb^{2+}, Cd^{2+}, and Zn^{2+} with aragonite and calcite mollusk shell [27]. As illustrated in the figure, the removal efficiency increased as the sorbent dosage was increased. Contrarily, it is well understood that adsorption capacity of a sorbent decreases as the sorbent dosage increases since only part of active adsorption sites is used [40–42]. Although the adsorption capacities of both metals were found high at lower dosages, the removal efficiency of Cd^{2+} was very low. The removal efficiency of Pb^{2+} remained almost indistinguishably constant (97.5–99.5%) while the sorption capacity decreased from 1007.5 mg/g to 202 mg/g with increasing the sorbent dosage from 0.1 g/L to 0.5 g/L. The removal efficiency of Cd^{2+} increased from 41.7% to 86%, while the sorption capacity decreased from 500 mg/g to 180 mg/g with the same increase in dosage. The high sorption of Pb^{2+} than Cd^{2+} can be explained by the solubility constant Ksp in addition to other factors discussed later in the sorption mechanism section. The solubility constant Ksp of cerussite and otavite are 7.40×10^{-14} and 1.0×10^{-12}, respectively (as given later in Table 4). This indicates that cerussite is slightly insoluble than otavite which can be considered for the higher sorption of Pb^{2+} on synthesized aragonite than Cd^{2+}. One paper studied the sorption of Pb^{2+} by calcite and aragonite with sizes of 100–200 um or less [43]. It was reported that the sorption of Pb^{2+} on calcite is higher than aragonite for sizes of 100–200 m, whereas for the smaller size of sorbents, the opposite was found to be true. This result was also found by another study for the sorption of Cd^{2+} and Pb^{2+} with aragonite and calcite [27]. However, in the current study, the sorption of Pb^{2+} on aragonite was also found to be as high as that of calcite. This might be due to the smaller size of the sorbent with a high surface area.

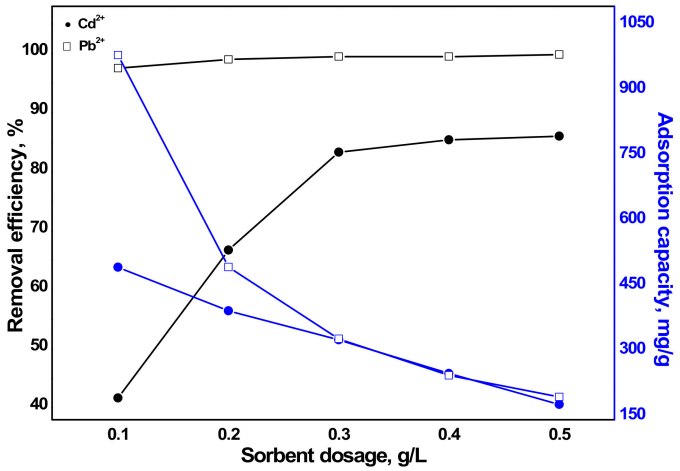

Figure 7. Influence of sorbent dosage on the removal efficiency and sorption capacity of metals by aragonite (condition: Cd^{2+} and Pb^{2+} concentration = 100 mg/L and pH = 5.8).

3.4. Influence of Initial pH

Another important parameter that influences adsorption capacity of a sorbent is the initial pH. The initial pH of a solution can affect the sorbent surface charge and the speciation of sorbates on the surface of the sorbent. The influence of initial pH on the sorption capacity of the metals by aragonite is presented Figure 8. The initial pH of 200 mL heavy metal-containing solution was adjusted to 2–6 with Cd^{2+} and Pb^{2+} concentration of 100 mg/L and 60 mg of aragonite to investigate the influence of pH on sorption capacity. At pH 2, H^{+} is released and competes with the metal ions (Cd^{2+} and Pb^{2+}) for the same active sorption sites resulting in negligible sorption capacity for both metals [44]. As pH > 2, the amount of adsorbed ions by aragonite started increasing rapidly. Although the sorption capacities at pH > 4 were all high, it reached a maximum capacity of 333.3 mg/L for Cd^{2+} and 335.8 mg/L for Pb^{2+} at pH 6.

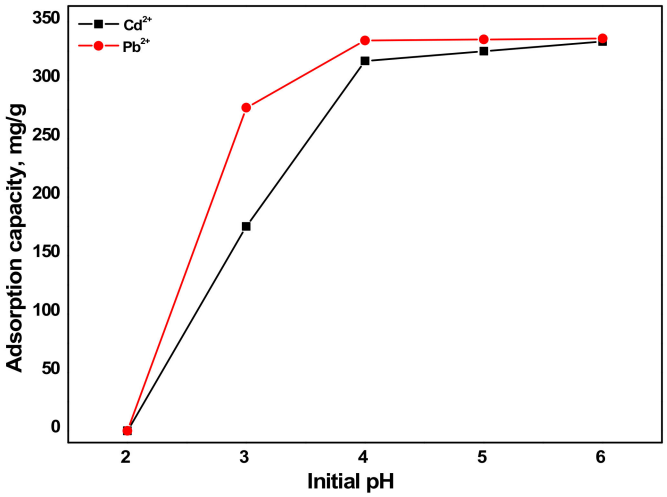

Figure 8. Influence of initial pH on the sorption capacity of metals by aragonite (condition: Cd^{2+} and Pb^{2+} concentration = 100 mg/L and sorbent dosage = 0.3 g/L).

3.5. Influence of Cd^{2+} and Pb^{2+} Concentration

Three Cd^{2+} and Pb^{2+} concentrations were conducted on 200 mL solution with pH 6 and sorbent dosage 60 mg. The result, as given in Figure 9, depicted that the sorption capacity decreased as Cd^{2+} and Pb^{2+} concentration decreased for the same reason explained earlier for the influence of sorbent dosage. As the initial metal concentration decreases, only some part of the active adsorption site will be used due to less sorbate. Besides, the removal efficiency increases with a decrease in the initial metal concentration [45]. However, in this study, the removal efficiencies of the three metal concentrations were almost the same. This was because the sorbent dosage (0.3 g/L) used was higher for the lower Cd^{2+} and Pb^{2+} concentrations (10 mg/L and 50 mg/L). Therefore, the effect on the removal efficiency was checked with a lower sorbent dosage (0.1 g/L) as presented in Figure 10. As a result, Pb^{2+} showed only a slight decrease in removal efficiency with an increase in Cd^{2+} and Pb^{2+} concentration since Pb^{2+} was easily removed even at lower dosages as discussed earlier. Furthermore, Cd^{2+} has clearly proved that an increase in Cd^{2+} and Pb^{2+} concentration resulted in decreased removal efficiency.

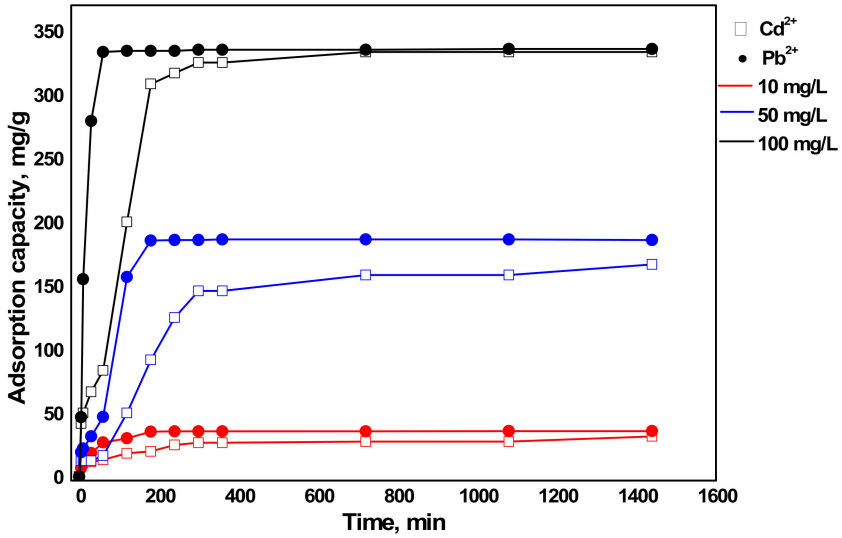

Figure 9. Influence of Cd^{2+} and Pb^{2+} concentration on the sorption capacity of metals by aragonite (condition: sorbent dosage = 0.3 g/L and pH = 6).

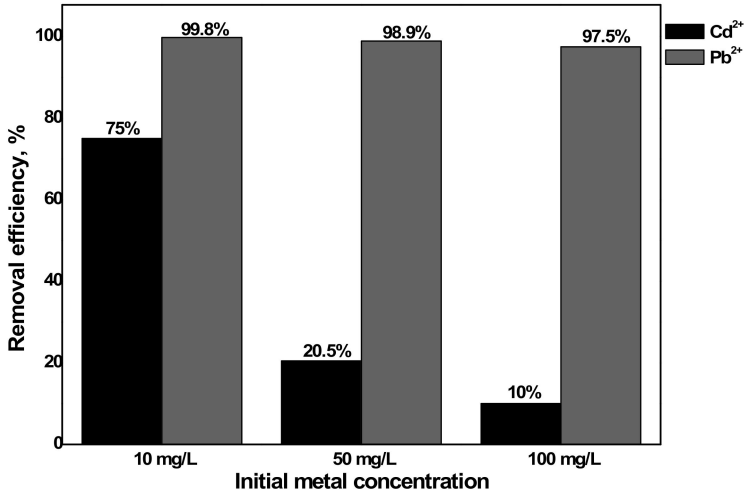

Figure 10. Influence of Cd^{2+} and Pb^{2+} concentration on the removal efficiency of metals by aragonite (condition: sorbent dosage= 0.1 g/L and pH = 6).

3.6. Sorption Isotherm

The sorption isotherm was modeled with the Langmuir and the Freundlich models, as given in Equations (5) and (6), respectively.

$$qe = \frac{\text{qmax} * \text{b} * \text{Ce}}{1 + \text{b} * \text{Ce}} \quad (5)$$

$$qe = K_f Ce^n \text{ , } \text{n} < 1 \quad (6)$$

where b is the Langmuir constant; q_{max} (mg/g) and q_e (mg/g) are the maximum and equilibrium adsorption capacity, respectively; C_e(mg/L) is the metal concentration in the solution at equilibrium; and k_f and n are the Freundlich empirical constants which measure adsorption capacity and intensity, respectively.

The two isotherm models fitted with the experimental data are given in Figure 11. The parameters of each model are also summarized in Table 3. The R^2 values with the Freundlich model were found to be slightly lower than Langmuir model. Therefore, the experimental data can be very well fitted with the Langmuir isotherm model.

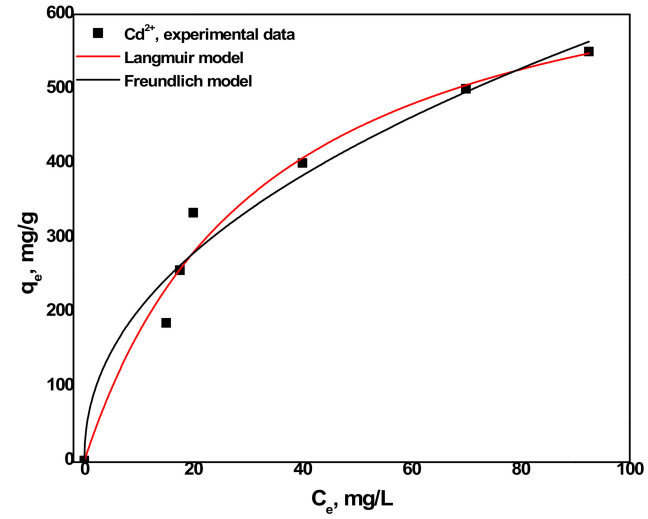

a)

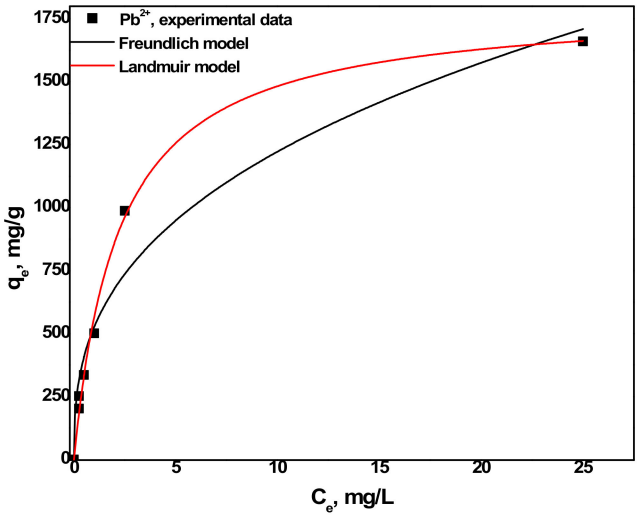

b)

Figure 11. (**a**) Langmuir and (**b**) Freundlich isotherm models of $Cd^{2+}$and Pb^{2+} sorption on aragonite.

Table 3. Isotherm model parameters of Cd^{2+} and Pb^{2+} sorption on aragonite.

Metal	Langmuir Isotherm Model Parameters			Freundlich Isotherm Model Parameters		
	q_{max} (mg g^{-1})	b	R^2	K_f (mg $^{1-1/n}$ g^{-1} $L^{1/n}$)	1/n	R^2
Cd^{2+}	743.59	0.031	0.986	70.499	0.404	0.972
Pb^{2+}	1807.9	0.454	0.995	526.88	0.326	0.955

3.7. Sorption Mechanism

XRD analysis of sorbent after exposed to 100 mg/L of Cd^{2+} and Pb^{2+} for 12 h is shown in Figure 12a. The possible phases to be formed were otavite, cerussite, hydrocerussite, and lead hydroxide [27]. However, metal hydroxides were not identified in the XRD patterns since they are not stable in the presence of carbonates. Cerussite and otavite were identified as major peaks with a minor phase of aragonite. An SEM image of the sorbent after exposure to 100 mg/L of Pb^{2+} and Cd^{2+} is also presented

in Figure 12b. The image showed an appearance of secondary layer on the surface of the sorbent, indicating that surface precipitation has taken place during sorption.

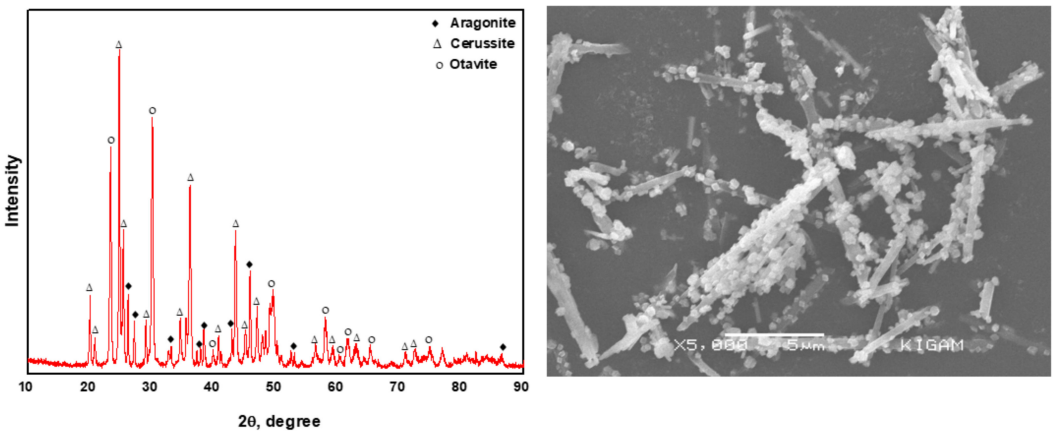

Figure 12. (**a**) X-ray diffraction pattern and (**b**) SEM image of sorbent after sorption.

Three possible processes can be involved at the $CaCO_3$-water interface: Dissolution, sorption and nucleation (crystal growth). The slightly acidic solution (pH = 6), resulted in the dissolution of $CaCO_3$ and released CO_3^{-2} (Equation (7)). Sorption of Cd^{2+} and Pb^{2+} also occurred in parallel with the dissolution aragonite (Equation (8)). Then nucleation (crystal growth) of cerussite and otavite resulted where the two metals ions reacted with the released CO_3^{-2} (Equation (9)).

$$CaCO_3(s) \rightarrow Ca^{2+} + CO_3^{-2} \quad (7)$$

$$CaCO_3(s) + Pb^{2+} + Cd^{2+} + CO_3^{-2} \rightarrow (Cd, Pb)CO_3 + Ca^{2+} \quad (8)$$

$$Pb^{2+} + Cd^{2+} + CO_3^{-2} \rightarrow (Cd, Pb)CO_3(s) \quad (9)$$

It has been argued that the mechanism of sorption when heavy metals interact with $CaCO_3$ could be ion exchange, surface precipitation as carbonate and hydroxycarbonate phases, complexation, and adsorption [27,36,43,46]. The similarity of ionic radii of ions favors the mechanism ion exchange where one ion potentially substitutes another similar ion. As presented in Table 4, the ionic radius of the metals Cd^{2+} and Pb^{2+} are different from those of Ca^{2+} in aragonite, which is evidence that a removal mechanism other than ion exchange is involved. Surface precipitation takes place with the dissolution of sorbents and precipitation of compounds on the surface of the sorbent. In this study, dissolution of aragonite took place continuously and metals (Cd^{2+} and Pb^{2+}) were sorbed where cerussite and otavite precipitated on the surface of aragonite crystals. Therefore, the removal mechanism was dominated by surface precipitation.

Lattice matching is an important factor for the formation of a layer on the substrate without defects. Aragonite and cerussite have similar crystal systems (orthorhombic) and small lattice mismatches, which can result in the epitaxial growth of cerussite, whereas otavite has a trigonal crystal system that is different from aragonite, resulting in precipitation of otavite in three-dimensional prismatic crystals on the surface of aragonite.

Table 4. Characteristics of possible compounds formed on the surface of the sorbent.

Metal	Ionic Radius (Å)	Hydration Energy (kJ/mol)	Carbonate	K_{sp} (25 °C)	Crystal System	Lattice Constants (Å)
Ca^{2+}	1.18, CN=9	−1592	Aragonite ($CaCO_3$)	6.0×10^{-9}	Orthorhombic	a = 4.959, b = 7.968, c = 5.741
Pb^{2+}	1.35, CN=9	−1481	Cerussite ($PbCO_3$)	7.40×10^{-14}	Orthorhombic	a = 5.195, b = 8.436, c = 6.152
			Hydrocerussite ($Pb_3(CO_3)_2(OH)_2$)	5.0×10^{-43}	Trigonal	a = b = 5.24, c = 23.74
Cd^{2+}	0.95, CN=6	−1807	Otavite ($CdCO_3$)	1.0×10^{-12}	Trigonal	a = b = 4.912, c = 16.199

4. Conclusions

Municipal solid waste such as eggshells is a threat to a sustainable environment. However, it can be converted into valuable material like aragonite and used in versatile applications, such as a filler paper and plastics. In the present study, eggshell (mainly composed of $CaCO_3$, calcite) was used as a precursor for the synthesis of aragonite through wet carbonation and applied to the removal of Cd^{2+} and Pb^{2+}. The conversion of calcite (eggshell) to aragonite is a vital process due to the inefficiency of calcite to remove Cd^{2+}. The influence of various factors was presented in this study. The sorption kinetics and isotherm were also investigated through systematic studies where the pseudo-second-order and Langmuir model well fitted the experimental data. The heavy metals were removed by surface precipitation mechanism where cerussite and otavite were precipitated out on the surface of the sorbent. All results demonstrate the effective and sustainable removal of toxic heavy metals by aragonite synthesized from eggshells. Therefore, eggshells can be a good substitute material of natural $CaCO_3$ for mitigating the contamination of water bodies with toxic heavy metals.

Author Contributions: Conceptualization, data curation, methodology, writing-original draft, L.H.; Visualization, software, N.S. and M.D.K.; Supervision, T.T.; Project administration, supervision, writing—review and editing, J.W.A. All authors have read and agreed to the published version of the manuscript.

Funding: This research was supported by the National Strategic Project-Carbon upcycling of the National Research Foundation of Korea (NRF) funded by the Ministry of Science and ICT (MSIT), the Ministry of environment (ME), and the Ministry of Trade, Industry, and Energy (MOTIE) (2017M 3D 8A 2084752).

Conflicts of Interest: The authors declare no conflicts of interest.

References

1. Gomes, M.G.; Pasquini, D. Utilization of eggshell waste as an adsorbent for dry purification of biodiesel. *Environ. Prog. Sustain.* **2018**, *37*, 2093–2099. [CrossRef]
2. Amanda, L.; Adriana, L.; Mario, D. Eggshell waste as catalyst: A review. *J. Environ. Manag.* **2017**, *197*, 351–359. [CrossRef]
3. Cree, D.; Rutter, A. Sustainable Bio-Inspired Limestone Eggshell Powder for Potential Industrialized. *Applications* **2015**. [CrossRef]
4. Shiferaw, N.; Habte, L.; Thenepalli, T.; Ahn, J.W. Effect of eggshell powder on the hydration of cement paste. *Materials* **2019**, *12*, 2483. [CrossRef] [PubMed]
5. Hamideh, F.; Akbar, A. Application of eggshell wastes as valuable and utilizable products: A review. *Res. Agric. Eng.* **2018**, *64*, 104–114. [CrossRef]
6. Tizo, M.S.; Blanco, L.A.V.; Cagas, A.C.Q.; Cruz, B.R.B.D.; Encoy, J.C.; Gunting, J.V.; Arazo, R.O.; Mabayo, V.I.F. Efficiency of calcium carbonate from eggshells as an adsorbent for cadmium removal in aqueous solution. *Sustain. Environ. Res.* **2018**, *28*, 326–332. [CrossRef]
7. Baláž, M.; Bujňáková, Z.; Baláž, P.; Zorkovská, A.; Danková, Z.; Briančin, J. Adsorption of cadmium(II) on waste biomaterial. *J. Colloid Interface Sci.* **2015**, *454*, 121–133. [CrossRef]
8. Meena, A.K.; Mishra, G.K.; Rai, P.K.; Rajagopal, C.; Nagar, P.N. Removal of heavy metal ions from aqueous solutions using carbon aerogel as an adsorbent. *J. Hazard. Mater.* **2005**, *122*, 161–170. [CrossRef]

9. Malar, S.; Vikram, S.S.; Favas, P.J.C.; Perumal, V. Lead heavy metal toxicity induced changes on growth and antioxidative enzymes level in water hyacinths [Eichhornia crassipes (Mart.)]. *Bot. Stud.* **2016**, *55*, 1–11. [CrossRef]
10. Boparai, H.K.; Joseph, M.; O'carroll, D.M. Kinetics and thermodynamics of cadmium ion removal by adsorption onto nano zerovalent ion particles. *J. Hazard. Mater.* **2011**, *186*, 458–465. [CrossRef]
11. Argun, M.E.; Dursun, S.; Ozdemir, C.; Karatas, M. Heavy metal adsorption by modified oak sawdust: Thermodynamics and kinetics. *J. Hazard. Mater.* **2007**, *141*, 77–85. [CrossRef] [PubMed]
12. Ali, R.M.; Hamad, H.A.; Hussein, M.M.; Malash, G.F. Potential of using green adsorbent of heavy metal removal from aqueous solutions: Adsorption kinetics, isotherm, thermodynamic, mechanism and economic analysis. *Ecol. Eng.* **2016**, *91*, 317–332. [CrossRef]
13. Uddin, M.K. A review on the adsorption of heavy metals by clay minerals, with special focus on the past decade. *Chem. Eng. J.* **2017**, *308*, 438–462. [CrossRef]
14. Ihsanullah Abbas, A.; Al-Amer, A.M.; Laoui, T.; Al-Marri, M.J.; Nasser, M.S.; Khraisheh, M.; Atieh, M.A. Heavy metal removal from aqueous solution by advanced carbon nanotubes: Critical review of adsorption applications. *Sep. Purif. Technol.* **2016**, *157*, 141–161. [CrossRef]
15. Demirbas, A. Heavy metal adsorption onto agro-based waste materials: A review. *J. Hazard. Mater.* **2008**, *157*, 220–229. [CrossRef]
16. Inyang, M.I.; Gao, B.; Yao, Y.; Xue, Y.; Zimmerman, A.; Mosa, A.; Pullammanappallil, P.; Ok, Y.S.; Cao, X. A review of biochar as a low-cost adsorbent for aqueous heavy metal removal. *Crit. Rev. Environ. Sci. Technol.* **2016**, *46*, 406–433. [CrossRef]
17. Park, H.J.; Jeong, S.W.; Yang, J.K.; Kim, B.G.; Lee, S.M. Removal of heavy metals using waste eggshell. *J. Environ. Sci.* **2007**, *19*, 1436–1441. [CrossRef]
18. Kobya, M.; Demirbas, E.; Senturk, E.; Ince, M. Adsorption of heavy metal ions from aqueous solutions by activated carbon prepared from apricot stone. *Bioresour. Technol.* **2005**, *96*, 1518–1521. [CrossRef]
19. Matlock, M.M.; Howerton, B.S.; Atwood, D.A. Chemical precipitation of heavy metals from acid mine drainage. *Water Res.* **2002**, *36*, 4757–4764. [CrossRef]
20. Fu, F.; Xie, L.; Tang, B.; Wang, Q.; Jiang, S. Application of a novel strategy-Advanced Fenton-chemical precipitation to the treatment of strong stability chelated heavy metal containing wastewater. *Chem. Eng. J.* **2012**, *189*, 283–287. [CrossRef]
21. Ma, L.; Wang, Q.; Islam, S.M.; Liu, Y.; Ma, S.; Kanatzidis, M.G. Highly Selective and Efficient Removal of Heavy Metals by Layered Double Hydroxide Intercalated with the MoS42-Ion. *J. Am. Chem. Soc.* **2016**, *138*, 2858–2866. [CrossRef] [PubMed]
22. Kurniawan, T.A.; Chan, G.Y.S.; Lo, W.H.; Babel, S. Physico-chemical treatment techniques for wastewater laden with heavy metals. *Chem. Eng. J.* **2006**, *118*, 83–98. [CrossRef]
23. Meunier, N.; Drogui, P.; Montané, C.; Hausler, R.; Mercier, G.; Blais, J.F. Comparison between electrocoagulation and chemical precipitation for metals removal from acidic soil leachate. *J. Hazard. Mater.* **2006**, *137*, 581–590. [CrossRef] [PubMed]
24. Polat, H.; Erdogan, D. Heavy metal removal from waste waters by ion flotation. *J. Hazard. Mater.* **2007**, *148*, 267–273. [CrossRef]
25. Zewail, T.M.; Yousef, N.S. Kinetic study of heavy metal ions removal by ion exchange in batch conical air spouted bed. *Alex. Eng. J.* **2015**, *54*, 83–90. [CrossRef]
26. Li, Y.; Xu, Z.; Liu, S.; Zhang, J.; Yang, X. Molecular simulation of reverse osmosis for heavy metal ions using functionalized nanoporous graphenes. *Comput. Mater. Sci.* **2017**, *139*, 65–74. [CrossRef]
27. Du, Y.; Lian, F.; Zhu, L. Biosorption of divalent Pb, Cd and Zn on aragonite and calcite mollusk shells. *Environ. Pollut.* **2011**, *159*, 1763–1768. [CrossRef]
28. Van, H.T.; Nguyen, L.H.; Nguyen, V.D.; Nguyen, X.H.; Nguyen, T.H.; Nguyen, T.V.; Vigneswaran, S.; Rinklebe, J.; Tran, H.N. Characteristics and mechanisms of cadmium adsorption onto biogenic aragonite shells-derived biosorbent: Batch and column studies. *J. Environ. Manag.* **2019**, *241*, 535–548. [CrossRef]
29. Flores-Cano, J.V.; Leyva-Ramos, R.; Mendoza-Barron, J.; Guerrero-Coronado, R.M.; Aragón-Piña, A.; Labrada-Delgado, G.J. Sorption mechanism of Cd(II, from water solution onto chicken eggshell. *Appl. Surf. Sci.* **2013**, *276*, 682–690. [CrossRef]
30. Setiawan, B.D.; Rizqi, O.; Brilianti, N.F.; Wasito, H. Nanoporous of waste avian eggshell to reduce heavy metal and acidity in water. *Sustain. Chem. Pharm.* **2018**, *10*, 163–167. [CrossRef]

31. Seo, K.S.; Han, C.; Wee, J.H.; Park, J.K.; Ahn, J.W. Synthesis of calcium carbonate in a pure ethanol and aqueous ethanol solution as the solvent. *J. Cryst. Growth.* **2005**, *276*, 680–687. [CrossRef]
32. Li, H.Y.; Tan, Y.Q.; Zhang, L.; Zhang, Y.X.; Song, Y.H.; Ye, Y.; Xia, M.S. Bio-filler from waste shellfish shell: Preparation, characterization, and its effect on the mechanical properties on polypropylene composites. *J. Hazard. Mater.* **2012**, *217–218*, 256–262. [CrossRef] [PubMed]
33. Du, Y.; Zhu, L.; Shan, G. Removal of Cd 2+ from contaminated water by nano-sized aragonite mollusk shell and the competition of coexisting metal ions. *J. Colloid Interface Sci.* **2012**, *367*, 378–382. [CrossRef] [PubMed]
34. Köhler, S.J.; Cubillas, P.; Rodríguez-Blanco, J.D.; Bauer, C.; Prieto, M. Removal of cadmium from wastewaters by aragonite shells and the influence of other divalent cations. *Environ. Sci. Technol.* **2007**, *41*, 112–118. [CrossRef] [PubMed]
35. Cubillas, P.; Köhler, S.; Prieto, M.; Causserand, C.; Oelkers, E.H. How do mineral coatings affect dissolution rates? An experimental study of coupled CaCO3 dissolution-CdCO3 precipitation. *Geochim. Cosmochim. Acta* **2005**, *69*, 5459–5476. [CrossRef]
36. Prieto, M.; Cubillas, P.; Fernández-Gonzalez, Á. Uptake of dissolved Cd by biogenic and abiogenic aragonite: A comparison with sorption onto calcite. *Geochim. Cosmochim. Acta* **2003**, *67*, 3859–3869. [CrossRef]
37. Habte, L.; Shiferaw, N.; Mulatu, D.; Thenepalli, T.; Chilakala, R.; Ahn, J.W. Synthesis of nano-calcium oxide fromwaste eggshell by sol-gel method. *Sustainability* **2019**, *11*, 3196. [CrossRef]
38. Chen, L.; Huang, F.; Li, S.; Shen, Y.; Xie, A.; Pan, J.; Zhang, Y.; Cai, Y. Biomimetic synthesis of aragonite superstructures using hexamethylenetetramine. *J. Solid State Chem.* **2011**, *184*, 2825–2833. [CrossRef]
39. Correia, L.M.; Cecilia, J.A.; Rodríguez-Castellón, E.; Cavalcante, C.L.; Vieira, R.S. Relevance of the Physicochemical Properties of Calcined Quail Eggshell (CaO) as a Catalyst for Biodiesel Production. *J. Chem.* **2017**, *2017*. [CrossRef]
40. Li, Y.; Du, Q.; Wang, X.; Zhang, P.; Wang, D.; Wang, Z.; Xia, Y. Removal of lead from aqueous solution by activated carbon prepared from Enteromorpha prolifera by zinc chloride activation. *J. Hazard. Mater.* **2010**, *183*, 583–589. [CrossRef]
41. Alghamdi, A.A.; Al-Odayni, A.B.; Saeed, W.S.; Al-Kahtani, A.; Alharthi, F.A.; Aouak, T. Efficient adsorption of lead (II), from aqueous phase solutions using polypyrrole-based activated carbon. *Materials* **2019**, *12*, 2020. [CrossRef] [PubMed]
42. Gupta, V.K.; Rastogi, A. Biosorption of lead from aqueous solutions by green algae Spirogyra species: Kinetics and equilibrium studies. *J. Hazard. Mater.* **2008**, *152*, 407–414. [CrossRef] [PubMed]
43. Godelitsas, A.; Astilleros, J.M.; Hallam, K.; Harissopoulos, S.A. Putnis, Interaction of calcium carbonates with lead in aqueous solutions. *Environ. Sci. Technol.* **2003**, *37*, 3351–3360. [CrossRef] [PubMed]
44. Miretzky, P.; Muñoz, C.; Carrillo-Chávez, A. Experimental binding of lead to a low cost on biosorbent: Nopal (Opuntia streptacantha). *Bioresour. Technol.* **2008**, *99*, 1211–1217. [CrossRef] [PubMed]
45. Sprynskyy, M.; Buszewski, B.; Terzyk, A.P.; Namieśnik, J. Study of the selection mechanism of heavy metal (Pb2+, Cu2+, Ni2+, and Cd2+) adsorption on clinoptilolite. *J. Colloid Interface Sci.* **2006**, *304*, 21–28. [CrossRef] [PubMed]
46. Fulghum, J.E.; Bryan, S.R.; Linton, R.W.; Bauer, C.F.; Griffis, D.P. Discrimination between Adsorption and Coprecipitation in Aquatic Particle Standards by Surface Analysis Techniques: Lead Distributions in Calcium Carbonates. *Environ. Sci. Technol.* **1988**, *22*, 463–467. [CrossRef]